Jurnal Kejuruteraan SI 3(1) 2020: 23-28
https://doi.org/10.17576/jkukm-2020-si3(1)-04

Investigating the Impact of Growth Temperature on WS_2 Thin Film

Md Khan Sobayel Bin Rafiq[a*], Afida Ayob[a], Badariah Bais[a], Md Akhtaruzzaman[b] & Nowshad Amin[c]

[a] *Department of Electrical, Electronic and Systems Engineering, Faculty of Engineering & Built Environment, Universiti Kebangsaan Malaysia, Malaysia*

[b] *Solar Energy Research Institute, Faculty of Engineering & Built Environment, Universiti Kebangsaan Malaysia, Malaysia*

[c] *Faculty of Engineering, University Tenaga Nasional,Malaysia*

**Corresponding author: akhtar@ukm.edu.my*

Received 27 January 2020, Received in revised form 15 April 2020
Accepted 15 May 2020, Available online 30 September 2020

ABSTRACT

Radio-frequency (RF) Magnetron Sputtering was used to deposit thin tungsten di sulfide (WS_2) films on top of soda lime glass substrates. Deposition temperature of RF magnetron sputtering was varied from room temperature (RT) to 200°C with 50°C interval to investigate the impact on film characteristics as well as to optimize for suitable application in thin film solar cells. Structural and opto-electronic properties of as-grown films were investigated and analyzed for different growth temperatures. All the WS_2 films exhibit granular structure consist of rhombohedral phase with a strong preferential orientation towards (101) crystal plane. Optical bandgaps are ranged from 1.73 eV to 2.3 eV for different growth temperatures. As-grown films show higher carrier concentration with n-type conductivity. Polycrystalline ultra-thin WS_2 film with bandgap of 2.4 eV, carrier concentration of 2.28 X 10^{17} cm^{-3} and resistivity of 1.52 Ω-cm were successfully achieved at 50°C with 50 W RF power that can be employed as window layers in thin film solar cells.

Keywords: Thin film; magnetron sputtering; photovoltaic; tungsten di sulphide; growth temperature

INTRODUCTION

In order to obtain economical thin film solar cells for a large-scale solar energy production, many conditions must be met by the absorbing semiconductor material in the device. First, the components should be cheap, non-toxic and abundant. Second, the material should have suitable optical and electrical characteristics such as an appropriate optical band gap, a high optical absorption coefficient, a high quantity yield for the excited carriers, a lengthy carrier diffusion distance, and a small recombination velocity in order to achieve high energy conversion efficiency. (Prasert Sinsermsuksakul et al. 2011) Transitional metal dichalcogenide (TMDC) have been a promising material for a large variety of applications for decades. It has drawn significant interest for its impressive performance in complex applications. Among the solar cell applicants there was a growing interest in thin film solar cell materials, particularly inexpensively, abundantly and non-toxically, tungsten di sulfide (WS_2). It has a strong anisotropy of optoelectrical properties due to the layered structure (Dickinson & Pauling, 1923). Although single crystals of this material have been studied extensively on optical devices, only some study of the photovoltaic characteristics of the thin film has been performed. TMDC in particular MoS_2 and WS_2 have raised the photovoltaic community's unique concern as absorber layer material in thin-film solar cells (Wyckoff 1963). This is due to their suitable bandgaps in the range of 1-2 eV as well as the very high absorption coefficient over 10^5 cm^{-1}(Etman et al. 1981; Pandey et al. 1996).

WS2 is still in the infancy of growth of thin film solar cells compared to other forms of solar cell components, such as Si, CdTe, CZTS, CIGS etc. At present, silicon solar cell technology, preceded by CdTe and CIGS, is the major driving force of solar photovoltaics. Yet Si solar technology's manufacturing costs are very high. The lack of supply of indium, high production costs of gallium and the issues with toxicity caused by Cd and Te have prompted researchers to look into low-cost, non-toxic and earth-rich materials into photovoltaic applications. In the last 30 years or so, TMDCs for solar cells with a fluid electrode is investigated as semiconductors (Bucher 1992; Sobayel et al 2018). WS_2 thin films have been prepared by various deposition techniques including chemical vapor deposition (CVD), magnetron sputtering, and vacuum evaporation and spray pyrolysis (Jäger-Waldau et al 1993, Regula et al. 1995; Hartnagel et al. 1995).

RF magnetron sputtering is a process of plasma-or ion-assisted deposition that bombards atoms to create thin film on substrate. Because of this highly energetic atomic bombardment, modifications in composition and bonding tend to happen (Ellmer 2008). This may have beneficial and harmful impacts for photovoltaic applications.

Therefore, deposition parameters play a significant role in the preferential sputtering development process (Rumaner et al. 1992). The growth temperature plays a major role to improve the film quality, enhance crystallinity and the device performance (Nisha et al. 2007; Canhola et al. 2005). This research has examined the morphological, structural and optoelectrical properties of the WS2 deposited by RF magnetron sputtering techniques under specific growth temperatures in order to analyze the effective application of WS2 in the solar cell.

METHODOLOGY

EXPERIMENT DESIGN AND PROCEDURE

In this study, WS_2 thin film was grown on soda-lime glass substrate by RF magnetron sputtering technique. All the deposition has been made in 60 minutes time. Soda lime glass substrates of 7.5 cm × 2.5 cm × 0.2 cm were used for film deposition. Phase cleaning procedures, including mechanical scrubbing, accompanied by acetone-methanol-deionized water in an ultrasonic bath and later dried with N2 gas flow were performed. As the source material, a 50 mm WS2 diameter (99.99 %) sputtering target (supplied by Kurt. J. Lesker) was used. Purging of the chamber carried out twice in order to remove unused components from the chamber. After that, the turbo-molecular pump took the chamber base pressure down to 10−6 torr. The working pressure was kept at 10-2 torr to instigate the plasma during the deposition. Substrate distance (sputter down) target and substratum holder rotation respectively were set at 8 cm and 10 rpm. In this study, growth temperature was varied from room temperature (RT) to 200°C. Deposition parameters used for this study are shown in table 1. During the deposition process, RF power was fixed at 50 W. All the samples were kept inside the sputtering chamber upon completion of the deposition until substrate temperature falls to room temperature as a measure to prevent as-grown films from being oxidized.

CHARACTERIZATION

As-grown films structural properties were examined by BRUKER aXS-D8 Advance CuKα diffractometer at room temperature. X-ray diffraction (XRD) patterns were recorded in the 2Θ range of 10° to 80° with a step size of 0.05° using Cu Kα radiation wavelength, λ= 0.15408 nm. To examine the surface pattern and roughness of the film, Atomic force microscopy (AFM) was used. Carl Zeiss Merlin field emission scanning electron microscope (FESEM) operated at 3 kV was used to observe grain size, surface morphology and cross-sectional view of the film. Electronic properties such as carrier concentration, mobility, and resistivity were measured by Hall Effect measurement system (HMS ECOPIA 3000) with a magnetic field of 0.57 T and probe current of 100 nA for all the samples. Absorption coefficient and bandgaps are calculated from Tauc plot.

TABLE 1. Sputtering parameters of the study

Parameter	Condition/Value
Target	WS_2 (99.9% pure)
Substrate	Soda Lime Glass
Base Pressure	3.0×10^{-6} Torr
Working Pressure	2.1×10^{-2} Torr
Deposition Time	60 min
Growth Temperature	RT, 50°C,100°C,150°C and 200°C
RF Power	50 W
Ar flow rate	4 sccm

RESULTS AND DISCUSSION

FILM MORPHOLOGY

It is already reported that growth rate has distinct relationship with growth temperature (Dongol et al. 2015). From FESEM, it has been found that at RT film thickness is very low. Moreover, it is revealed that as-deposited films exhibit amorphous properties at RT. Inter molecular bond and layered structure starts to form with the application of growth temperature. It is also found that film thickness increases sharply over 50°C and remains almost same between 100°C to 200°C growth temperature. Highest thickness of 308.6 nm WS_2 thin film has been obtained at 200oC growth temperature at lowest thickness of 102.8 nm has been observed at RT. Figure 1 represents the film thickness with respect to growth temperature for WS2 thin film. Figure 1(c) represents the relationship with growth temperature and growth rate of the film. Color in the figure 1(c)indicates the growth rate of the film.

Figure 2 shows the surface view of as-grown WS_2 thin films for different growth temperatures. All the films with growth temperature show smooth morphology and granular like structure. From FESEM surface image it clear that WS_2 thin film at RT is amorphous. With the increment of temperature, films start to form crystalline structure. And higher growth temperature, as-grown films exhibits dense and compact structure. Thus, it is revealed that growth temperature in sputtering process is pre-requisite to achieve dense microstructure and better crystallinity of WS_2 thin film.

STRUCTURAL ANALYSIS

Figure 3 shows the XRD pattern for as-sputtered WS_2 films of different temperature variations. It is found that film deposited at room temperature is amorphous in nature. The other films fabricated with different growth temperatures display two main peaks (101) and (112) showing the polycrystalline structure. The XRD patterns obtained in this analysis are consistent with the regular XRD pattern described in JCPDS. Films are found at 3R phase and also exhibit most intense peak at 2Θ = 34.38°

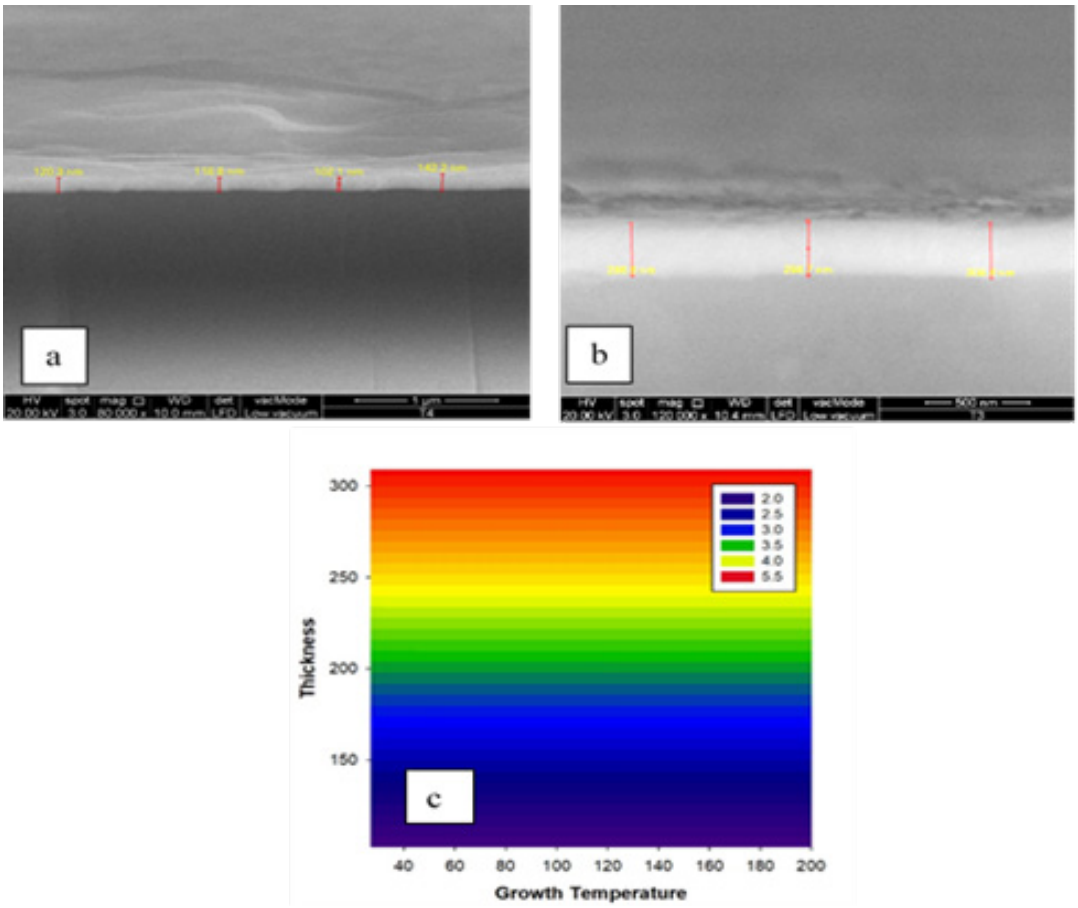

FIGURE 1. (a) Lowest thickness at RT (b) Highest thickness at 200°C (c) Effect of growth temperature on film thickness and film growth rate

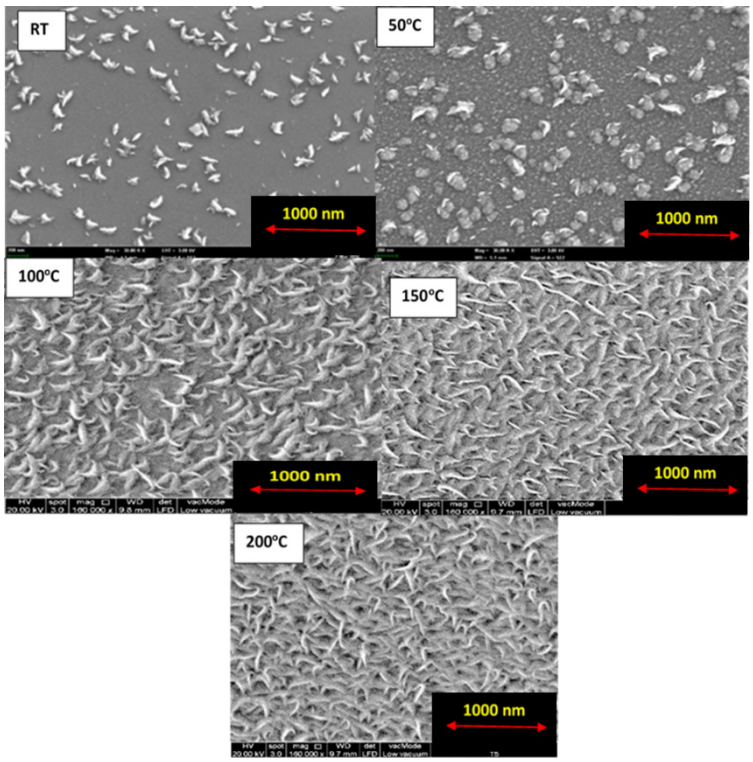

FIGURE 2. FESEM images of as grown WS_2 for different temperature variation

corresponding to (101) plane. From the growth temperature 100°C and above; peaks are found sharp and almost having same intensity. Below 100°C, peak intensity is less. It signifies that as-grown films need at least 100°C to achieve better crystallinity which completely agrees with the morphological analysis.

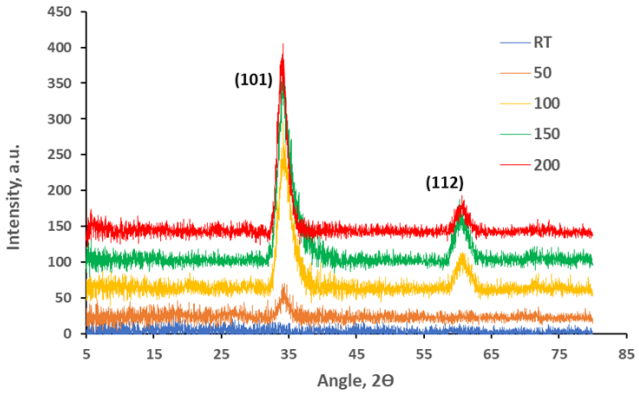

FIGURE 3. XRD patterns of WS_2 for various growth temperature

By using the Scherrer equation the average particle or crystallite size was determined (Scherrer et al. 1978).

$$L(hkl) = \frac{0.9\lambda}{\beta \cos\theta} \quad (1)$$

Where L, λ, β, Θ are the crystallite size, wavelength, FWHM and the angle between incident and scattering planes respectively. Crystalline size measured from 69.09 Å to 96.72 Å. Grains with different relative orientations, positions and phase variations create disparities as light waves are scattered by them. The large number of grains of various orientations displace the atom while the crystal arrays form (Sèmeh Jebli et al 2019). These array strains displace atoms from their original structure. It might happen because of high energy deposition. In fact, lower strain value means higher crystallinity (Koçak et al 2016). Strain has been calculated by following relation (Dhanam, M., et al. 2007).

$$\varepsilon = \frac{\beta}{4tan\theta} \quad (2)$$

Here, is the strain. The results of X-Ray Diffraction (XRD) measurements are shown in Table 2. The obtained values of crystallite size and strain at different growth temperatures are illustrated in Figure 4.

TABLE 2. XRD results for different growth temperature of WS_2

Temp, °C	d (h,k,l) Ă	Θ (rad)	FWHM (ß)	L, Ă	N, cm^{-2}	ε 10^{-2}	δ (10^4)
50	2.59	0.299	0.021	69.09	7.85	1.70	2.09
100	2.61	0.299	0.015	96.72	2.88	1.22	1.07
150	2.56	0.3	0.019	80.63	4.88	1.45	1.54
200	2.58	0.299	0.018	80.60	4.92	1.46	1.54

It is observed that there is a contradiction of behavior regarding crystallite size and strain with the increase of growth temperature. This is because, with the increase of growth temperature, carrier concentration increases. This phenomenon reduces structural defects and subsequently increases the crystallite size and improves film quality. Here, the highest crystallite size and lowest strain have been observed at 100°C. From this analysis it is revealed that as-grown WS_2 films show better crystallinity at 100°C growth temperature.

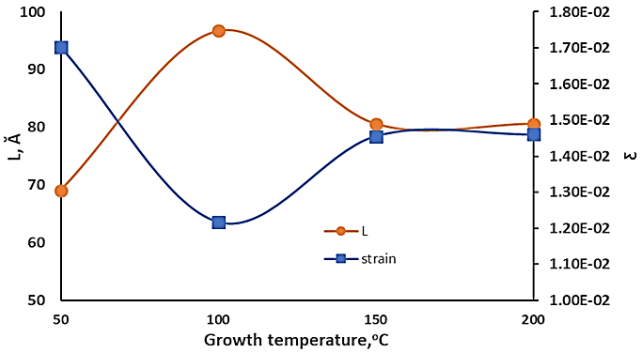

FIGURE 4. Effect of growth temperature on both crystallite size (L) and strain of WS_2 film

Dislocation density (δ) is another important factor for determining crystallographic properties of thin film. Dislocation is caused by the imperfections in crystal orientation. It is measured by Williamson and Smallman's relationship (Dhanam et al. 2009).

$$\delta = \frac{1}{L^2} \quad (3)$$

Here, δ is the dislocation density and L is crystallite size. It has been found that with the increase of growth temperature L increases; ε, δ and N decreases. At low growth temperature (< 100°C), crystallite size is very low (69.09 Ă). Again, at higher growth temperature (≥ 150°C), crystallite size remains almost the same and negligible change is observed while considering ε and δ on as-deposited WS_2 film. This was attributed to the fact that the growth temperature is essential to achieve crystallinity and greatly reduces but does not eliminate the defect density completely.

OPTICAL ANALYSIS

Optical behaviour of the as-deposited WS_2 thin films at various growth temperature are characterized by UV-VIS spectrometer. It is to be mentioned that, films deposited at RT are excluded for further investigation as initial results determines the non-suitability of the film for photovoltaic applications. Absorption coefficient has been determined by the Beer-Lambert law and represented in Figure 5.

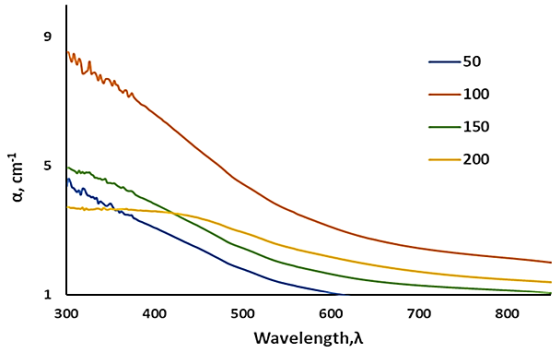

FIGURE 5. Absorption coefficient of WS_2 under different growth temperature

From the study, it has been revealed that highest absorbance of WS_2 thin film is at 100°C growth temperature and lowest at 50°C. Absorbance at growth temperature over 100°C and higher ranges from 280 nm to 800 nm wavelength. A Tauc plot usually shows the amount of the abscissa (light spectrum energy) and the sum $(\alpha hv)^{1/n}$ on the ordinate where α is the material absorption coefficient (Asif Ali Tahir et al 2009). The equation used to determine the band gap is as following:

$$\alpha hv = A\left(hv - Eg\right)\hat{}\, n \tag{4}$$

Here, α is the measured absorption coefficient (cm^{-1}) near the absorption edge, *A* is a constant, *hv* is photon energy (eV), *Eg* is optical band-gap (eV), *n* is a constant. The value of n is determined from the nature of optical transition. n=2 or 3 for indirect allowed and indirect forbidden transition, respectively and n=1/2 or 3/2 for direct allowed and direct forbidden transition, respectively.

The optical band gap of WS_2 for different growth temperatures has been evaluated by using Tauc plot depicted in Figure 6. It is revealed that optical band gap of as-deposited WS_2 are in the range of 1.8 eV to 2.4 eV for all variations of growth temperature. At the variations of 50°C growth temperature, bandgap is observed at 2.4 eV that suits for window layer in solar cell. Again, at growth temperature over 50°C, the optical band gap is found between 1.8 to 2.1 eV which is desirable bandgap for absorber materials. These results give strong push to put WS_2 as absorber layer material in solar cell devices.

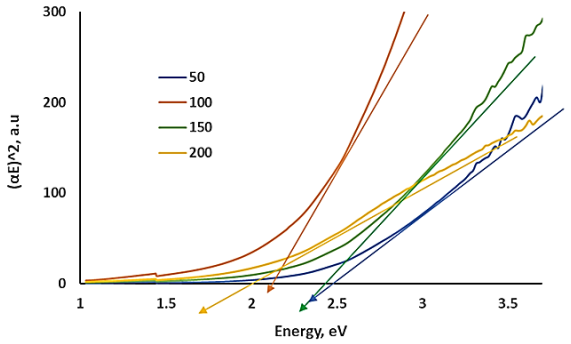

FIGURE 6. Determination of band gap of WS_2 by Tauc plot for growth temperature variation

ELECTRICAL PROPERTIES

Electrical properties of thin film determine is conductivity, resistivity and semiconducting nature (Schroder 1998). The properties of as-grown WS_2 films as a function of growth temperature were measured by Hall measurement and results are summarized (carrier concentration, hall mobility, resistivity and conductivity) in Table 3.

TABLE 3. Hall effect results of WS_2 for different growth temperature of WS_2

Growth Temp. (°C)	C.concentration (cm^{-3})	Hall Mobility (cm^2/V.s)	Resistivity (Ω-cm)	Conductivity type
50	2.58×10^{17}	0.945	1.52	n
100	6.84×10^{18}	1.9	1.65	n
150	8.85×10^{18}	2.335	2.54	n
200	2.31×10^{19}	1.872	0.591	n

It has been observed that carrier concentration and mobility of as-deposited films increase with the increase of growth temperature up to 150°C, but mobility starts to decrease at 200°C. Highest carrier concentration has been observed at 200°C with resistivity as low as 0.591 Ω-cm. Highest carrier mobility of 2.335 cm^2/V.s has been found at growth temperature of 150°C with carrier concentration of 8.85 X 10^{18} cm^{-3} . However, all the films exhibit n-type conductivity.

CONCLUSION

By examining all the characteristics of as-deposited WS_2 thin film with respect to various growth temperature, it can be concluded that WS_2 thin film cannot be deposited at RT for photovoltaic applications. Growth temperature range of 100°C to 150°C is suitable for depositing as absorber layer thin film. But the film n-type conductivity remains as the biggest challenge to utilize WS_2 as an absorber layer material. Interestingly, at 50°C growth temperature as-deposited WS_2 films shows optical bandgap of 2.4 eV with lower absorption coefficient and moderate carrier concentration (2.58 X 10^{17} cm^{-3}). This phenomenon indicates that WS_2 can be incorporated differently than absorber material in solar cells. However, as most of the parameters are well match with the absorber layer material, so more investigation and optimization on other parameters are required to develop WS_2 as photovoltaic absorber layer material.

DECLARATION OF COMPETING INTEREST

None.

ACKNOWLEDGEMENT

The authors would like to thank Universiti Kebangsaan Malaysia for their financial support under the grant DIP-2019-019.

REFERENCES

Asif Ali Tahir, K. G. 2009. Upul Wijayantha, Sina Saremi-Yarahmadi, Muhammad Mazhar & Vickie McKee, Nanostructured α-Fe2O3 Thin Films for Photoelectrochemical Hydrogen Generation. *Chemistry of Materials* 21 (16): 3763-3772.

Bucher, E. 1992. *Photo Electrochemistry and Photovoltaics of Layered Semiconductors*, edited by A. Aruchamy (Kluwer Academic Publishers, Dordrecht.

Canhola, P. et al. 2005. Role of annealing environment on the performances of large area ITO films produced by RF magnetron sputtering. *Thin Solid Films* 487: 271–276.

Dhanam, M. et al. 2009. Analysis of ZnS nanoparticles prepared by surfactant micelle-template inducing reaction. *Chalcogenide Letters* 12: 713-722

Dickinson, R. and Pauling, L. 1923. The crystal structure of molybdenite. *Journal of the American Chemical Society*, 45(6): 1466-1471. 10.1021/ja01659a020.

Dongol, M. et al. 2015. Thermal annealing effect on the structural and the optical properties of Nano CdTe films. *Optik* 126: 1352–1357.

Ellmer, K. 2008. Low temperature plasmas. fundamentals, technologies & techniques. *Wiley-VCH* 2: 675.

Etman, M., Tributsch, H. & Bucher, E. 1981. Photovoltages exceeding the band gap observed with WSe2/I− solar cells. *Journal of Applied Electrochemistry* 11(5): 653–660

Hartnagel, H. L., Dawar, A. L., Jain, A. K. & Jagadish, C. 1995. *Semiconducting Transparent Thin Films*. Bristol: Institute of Physics Publishing.

Jäger-Waldau, A., Lux-Steiner, M. C., Jäger-Waldau, and Bucher, E. 1993. *Appl. Surf. Sci.* 70/71: 731.

Koçak, Y. et al. 2016. *J. Phys.: Conf. Ser.* 707 012028.

Nisha, M. et al. 2005. Effect of substrate temperature on the growth of ITO thin films. *Applied Surface Science* 252: 1430–1435

Pandey, R. N., Chandra, K. S., Babu & Srivastava, O. N. 1996. High conversion efficiency photoelectrochemical solar cells. *Progress in Surface Science* 52(3): 125-192.

Prasert Sinsermsuksakul , Jaeyeong Heo , Wontae Noh , Hock, A. S. & Gordon, R. G. 2011. Atomic layer deposition of tin mono-sulfide thin films. *Adv. Energy Matter* 1: 1116–1125.

Regula, M., Ballif, C. and Lévy, F. 1995. *Polycrystalline Semiconductors IV – Physics, Chemistry and Technology*, edited by S. Pizzini, H. P. Strunk, and J. H. Werner. Switzerland: Trans Tech, Zug,.

Rumaner, L. E., Tazawa, T. & Ohuchi, F. S. 1992. Compositional change of (0001) WS_2 surfaces induced by ion beam bombardment with energies between 100 and 1500 eV. *J. Vac. Sci.Technol*. 12: 2451.

S. Singh et al. 2007. Effect of substrate temperature on the structure and optical properties of ZnO thin films deposited by reactive RF magnetron sputtering. *Thin Solid Films* 515: 8718–8722.

Scherrer et al. 1978. After sixty years: A survey & some new results in the determination of crystallite size. *J. Appl. Cryst.* 11: 102-113.

Schroder, D. K. 1998. *Semiconductor Material and Device Characterization*. Arizona: Arizona State University.

Sèmeh Jebli et al. 2019. Synthesis, crystal structure, Mössbauer spectroscopy, optical and magnetic properties of Cs2M2Fe(PO4)3 (M = Mn, Co, Ni, Cu) ordered pollucite structure. *Journal of Solid State Chemistry* 270: 265-272.

Sobayel, K. et al. 2018. Numerical modeling of high efficiency tungsten-di-sulfide (WS2) solar cells with various buffer layers by scaps-1D. *Chalcogenide Letters* 15(6).

Wyckoff, R. G. W. 1963. *Crystal Structures*. New York: Inter Science.